Illuminating the Active Universe: Multi-Wavelength and Multi-Messenger Insights into AGN

# X-ray Flare Evolution and Changing-Look Nature of the TeV Blazar OQ 334

**P. K. Navaneeth**
Janusz Gil Institute of Astronomy, University of Zielona Góra, Poland

## Outline

1. **Introduction**
2. **Timing & MWL Analysis**
3. **X-ray Analysis**
4. **Broad-band SED**
5. **Changing-Look States**
6. **Conclusion**

## Objectives

Using multi-wavelength observations with the focus on X-rays, we investigate:

- The spectral evolution of the X-ray flares and the emission components driving them.
- The X-ray behaviour across the transitions between the FSRQ and BL Lac states.

## Blazars

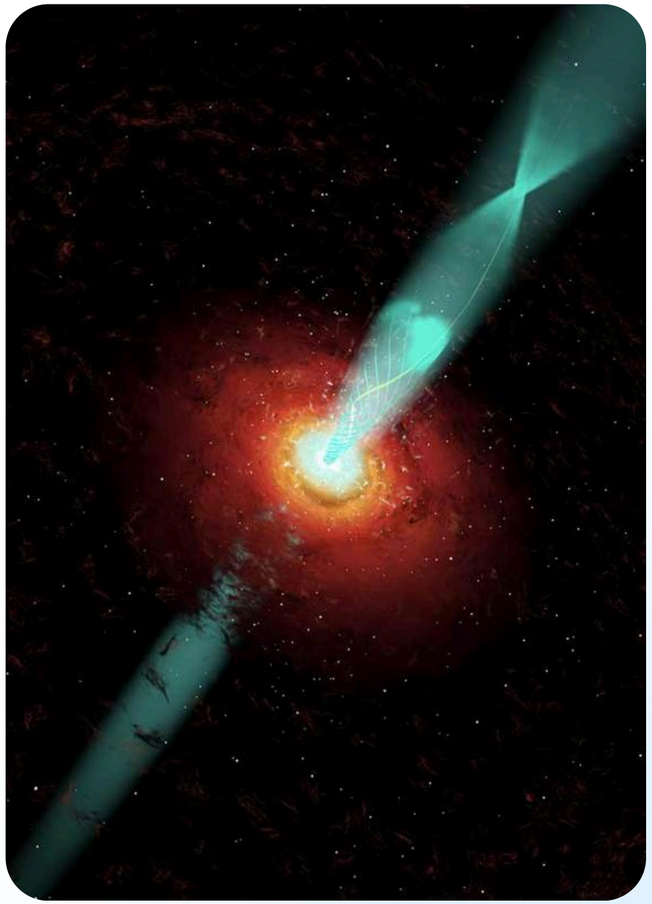
Two subclasses, classified by their optical spectra:

- **Flat Spectrum Radio Quasars (FSRQs)**

  Broad emission lines with rest-frame EW ≥ 5 Å

- **BL Lacertae objects (BL Lacs)**

  Weak or absent emission lines (rest-frame EW < 5 Å)



## Changing-Look Blazars (CLBs)

Sources that transition between the FSRQ and BL Lac classes across epochs, crossing the EW = 5 Å boundary.

# Changing-Look Blazars (CLBs)

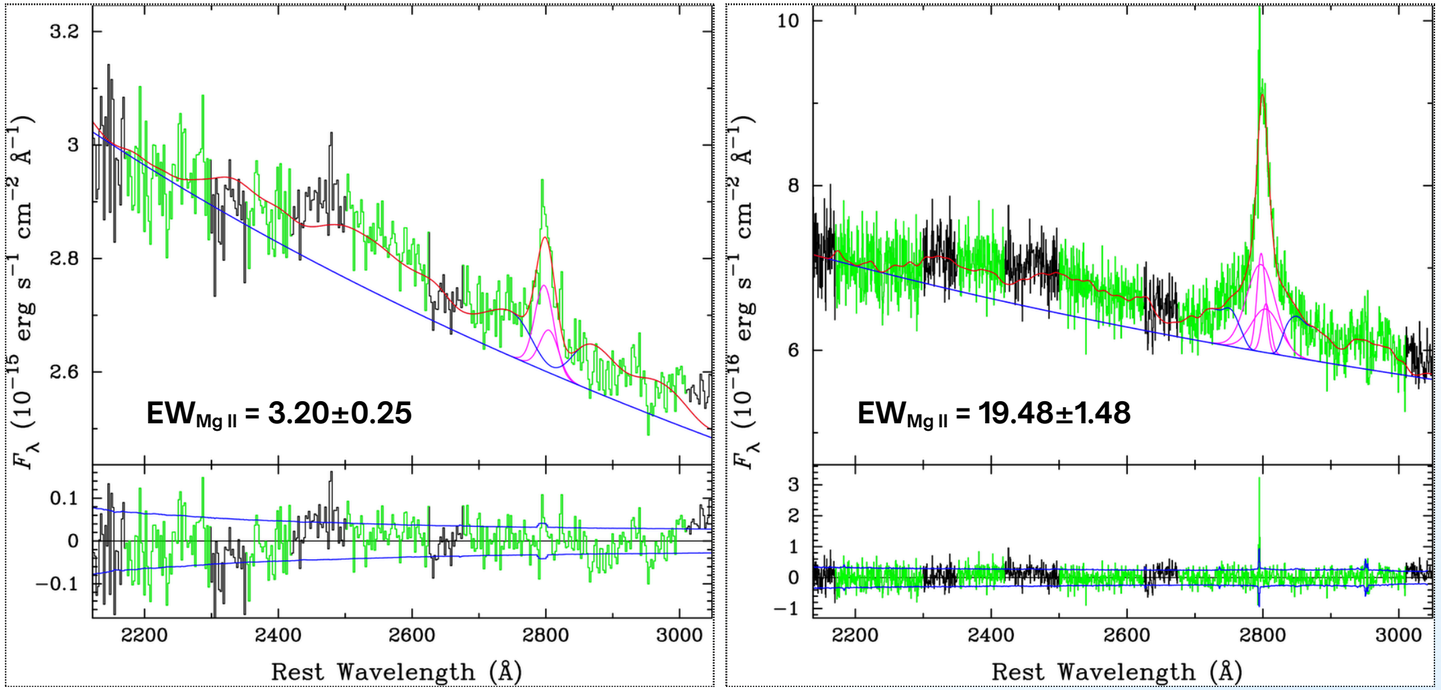
**OQ 334** (Misra et al. 2021)

**Ton 599** (Chen et al. 2025)

**OP 313** (Pandey et al. 2025)

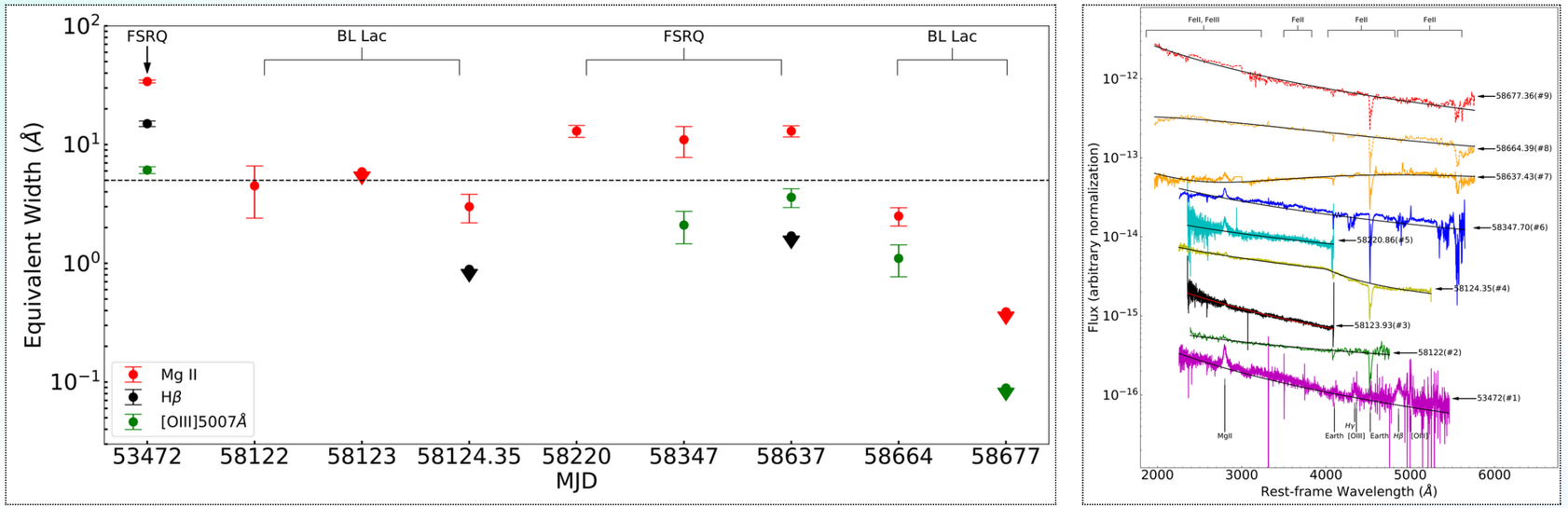
**PKS 0446+112** (Paiano et al. 2026)

**AO 0235+164** (Ren et al. 2026)




**Pandey et al. (2025)**

# OQ 334




**Misra et al. (2021)**

The γ-ray photon index ($\Gamma_\gamma$) shows different ranges for different states (**Ren et al. 2024**):

- **FSRQ state: $\Gamma_\gamma \gtrsim 2.2$**
- **Transition state: $2.0 < \Gamma_\gamma < 2.2$**
- **BL Lac state: $\Gamma_\gamma \lesssim 2.0$**

# MWL Lightcurve

MJD 54769.0 - 60824.0

↓

MJD 58095.0 - 60580.0

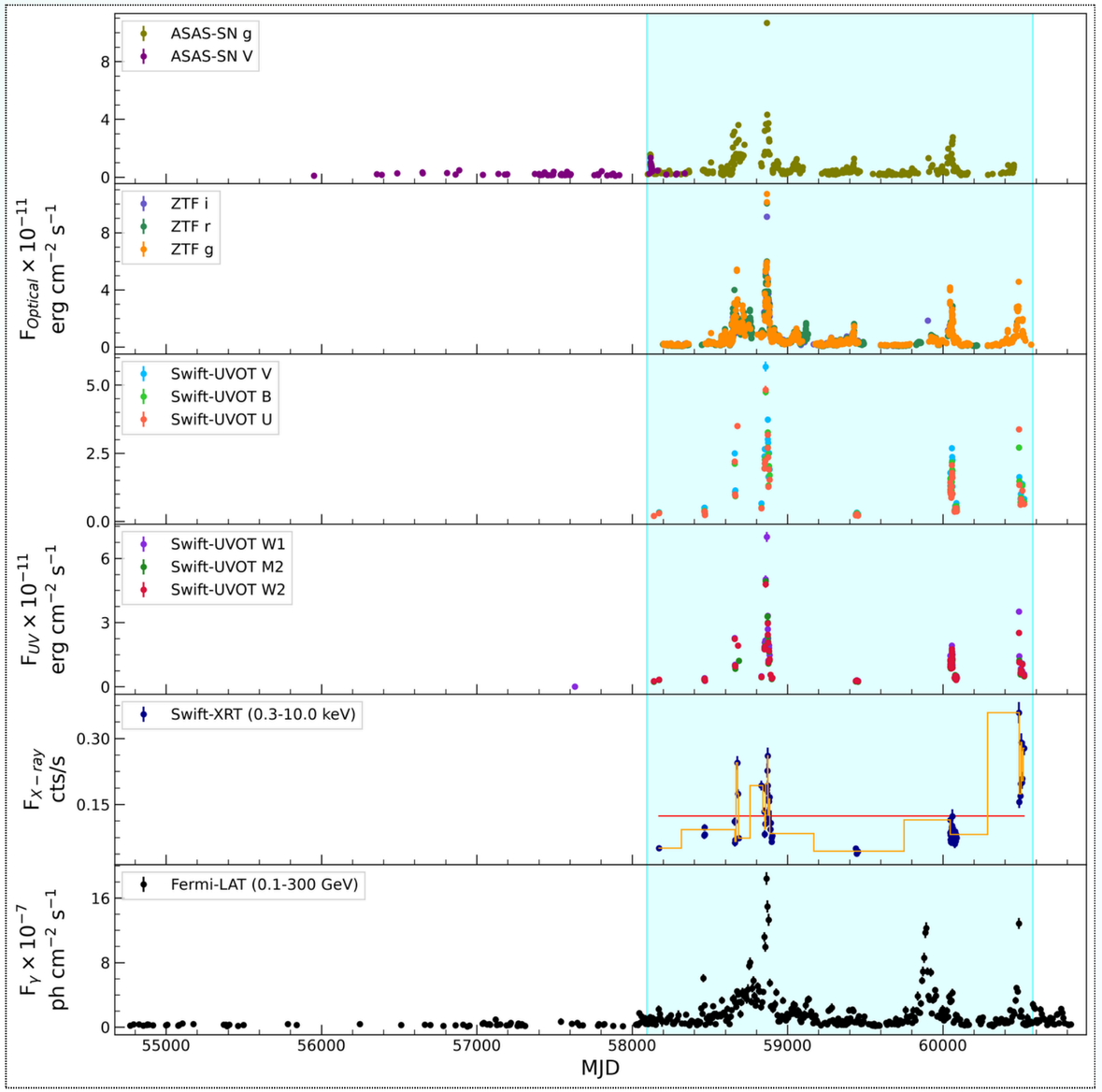
**ASAS-SN**

**ZTF**

**Swift-UVOT**

**Swift-XRT**

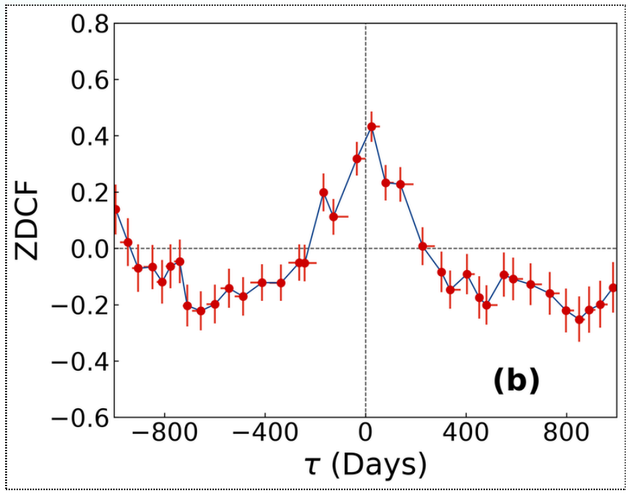
**Fermi-LAT**



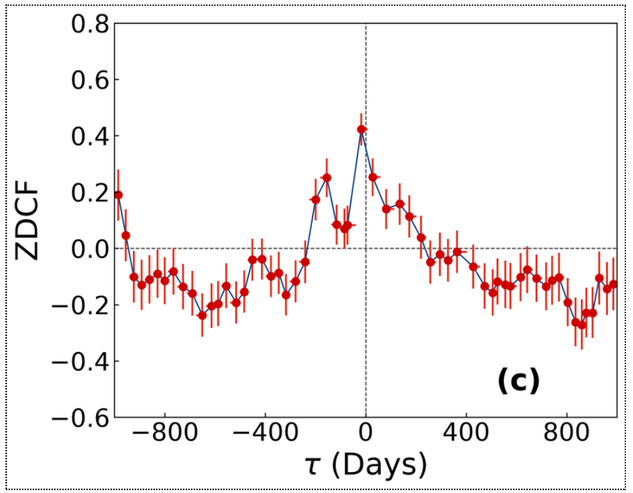
# Cross-Correlations

z-transformed Discrete Correlation Function (ZDCF)

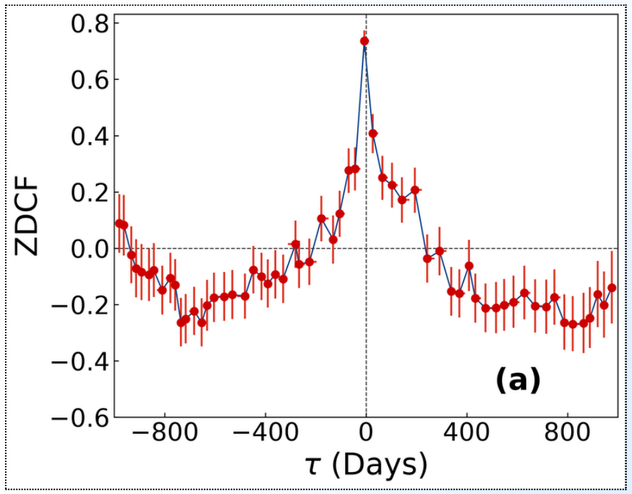
| LC Pair | Lag (days) | DCF |
|---|---|---|
| (a) Fermi-LAT vs ZTF-i | $-6.8$ | $0.73 \pm 0.03$ |
| (b) Fermi-LAT vs ZTF-r | 24.5 | $0.43 \pm 0.05$ |
| (c) Fermi-LAT vs ASAS-SN g | $-17.7$ | $0.42 \pm 0.05$ |




Fermi-LAT - ZTF r



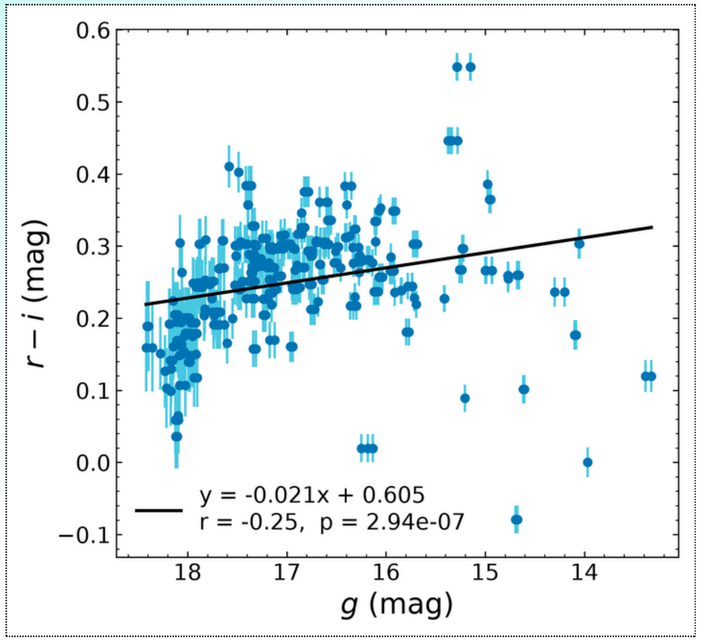

Fermi-LAT - ASAS-SN g

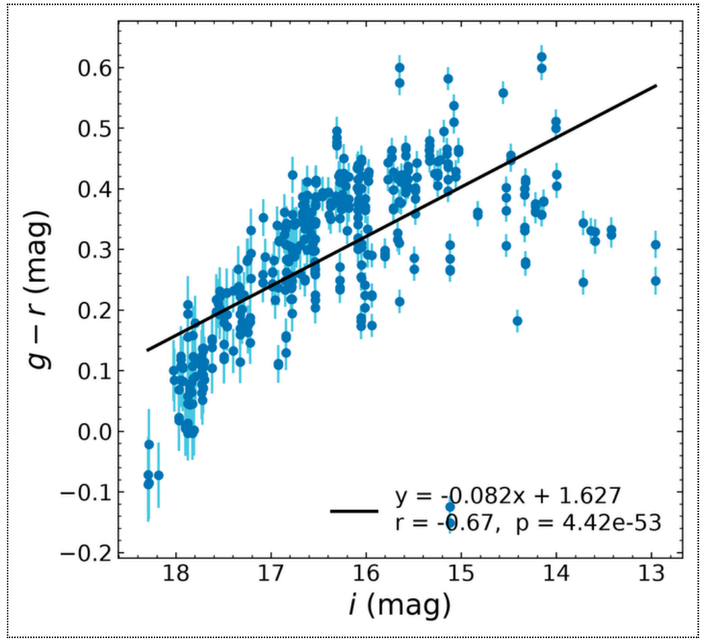


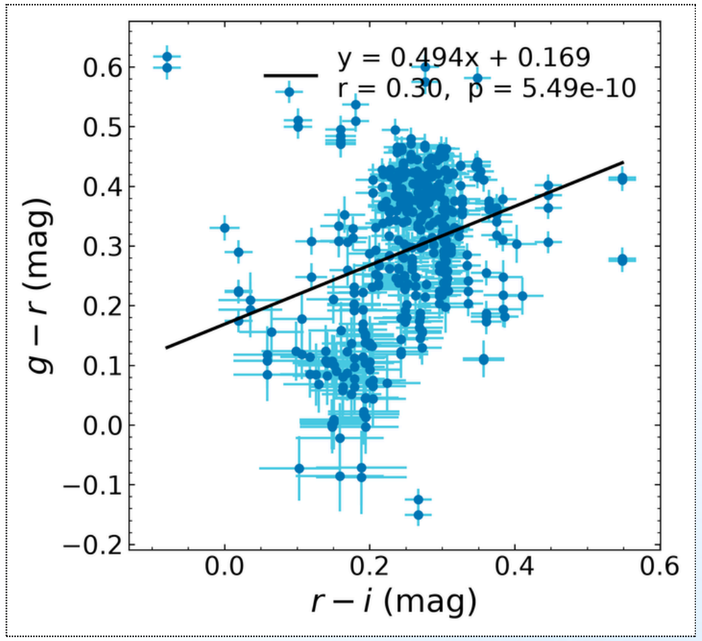

Fermi-LAT - ZTF i

# CMD & CCD

Colour-magnitude and colour-colour diagrams from ZTF g, r, i band photometry




Optical spectrum reddens as the source brightens: **redder-when-brighter (RWB)** behaviour

Colour changes are consistent across the optical bands

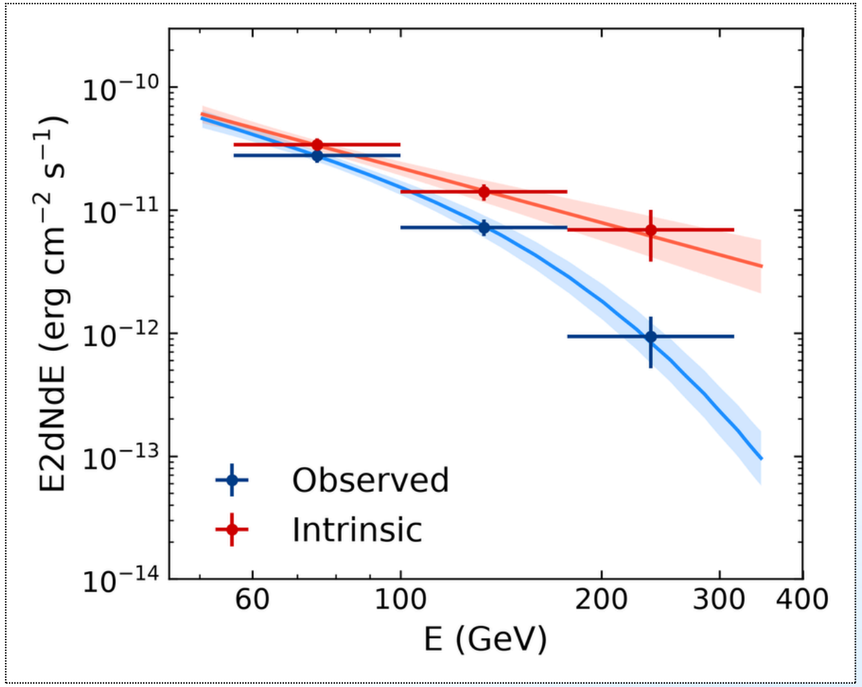
## VHE Emission

Data cover the VHE flare of MAGIC Collaboration et. al (2021), coinciding with flare X2.

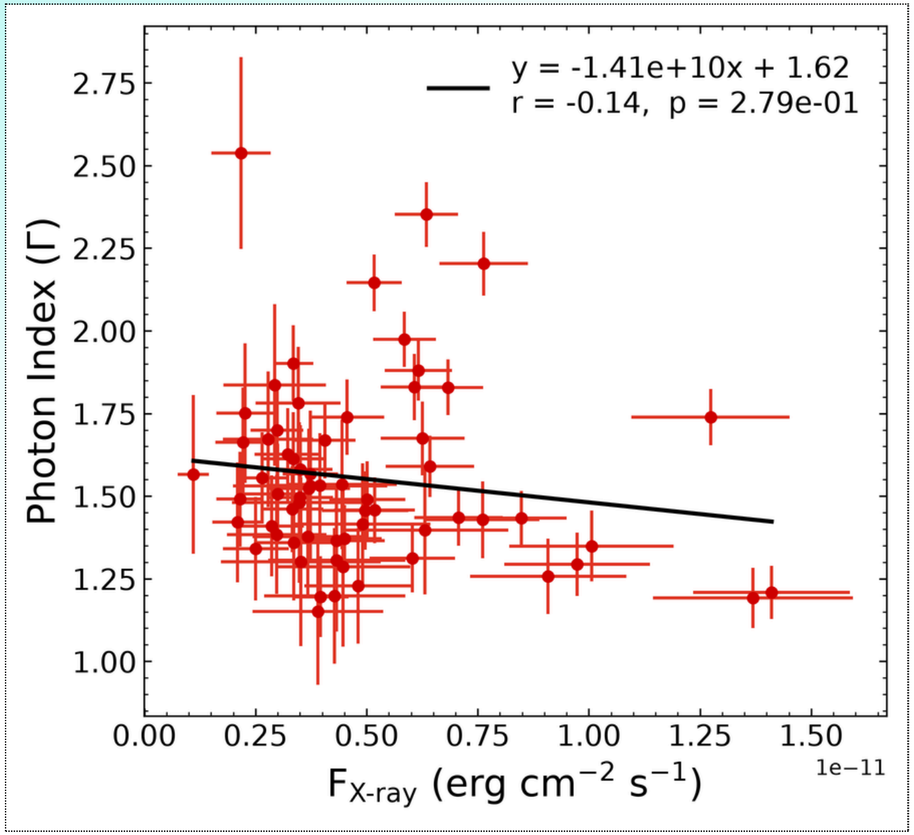
- MJD 58869.22 - 58885.25

Power law model with EBL absorption (Dominguez et al. 2011, z = 0.681)

$$\frac{\mathrm{d}N}{\mathrm{d}E} = N_0 \left( \frac{E}{E_0} \right)^{-\Gamma}$$



# X-ray Spectral Analysis




64 Swift-XRT observations over the studied period

Absorbed models with tbabs. $n_H = 1.08 \times 10^{20}$ cm$^{-2}$

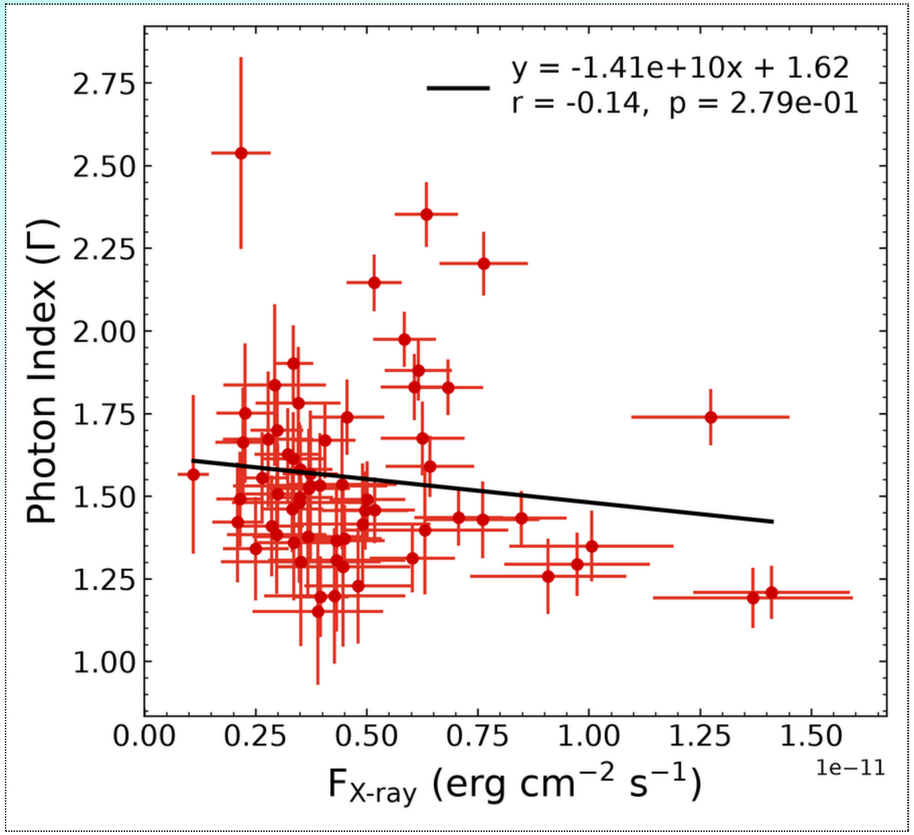
- tbabs*powerlaw
- tbabs*logpar
- tbabs*bknpower

$$\frac{dN}{dE} = K\,E^{-\Gamma}$$

$$\frac{dN}{dE} = K\left(\frac{E}{E_{\mathrm{p}}}\right)^{-\alpha-\beta\log(E/E_{\mathrm{p}})}$$

$$\frac{dN}{dE} = \begin{cases} K\,E^{-\Gamma_1} & E \le E_{\mathrm{b}} \\ K\,E_{\mathrm{b}}^{\Gamma_2-\Gamma_1}\,E^{-\Gamma_2} & E > E_{\mathrm{b}} \end{cases}$$

# X-ray Spectral Analysis




Corrected Akaike Information Criterion:

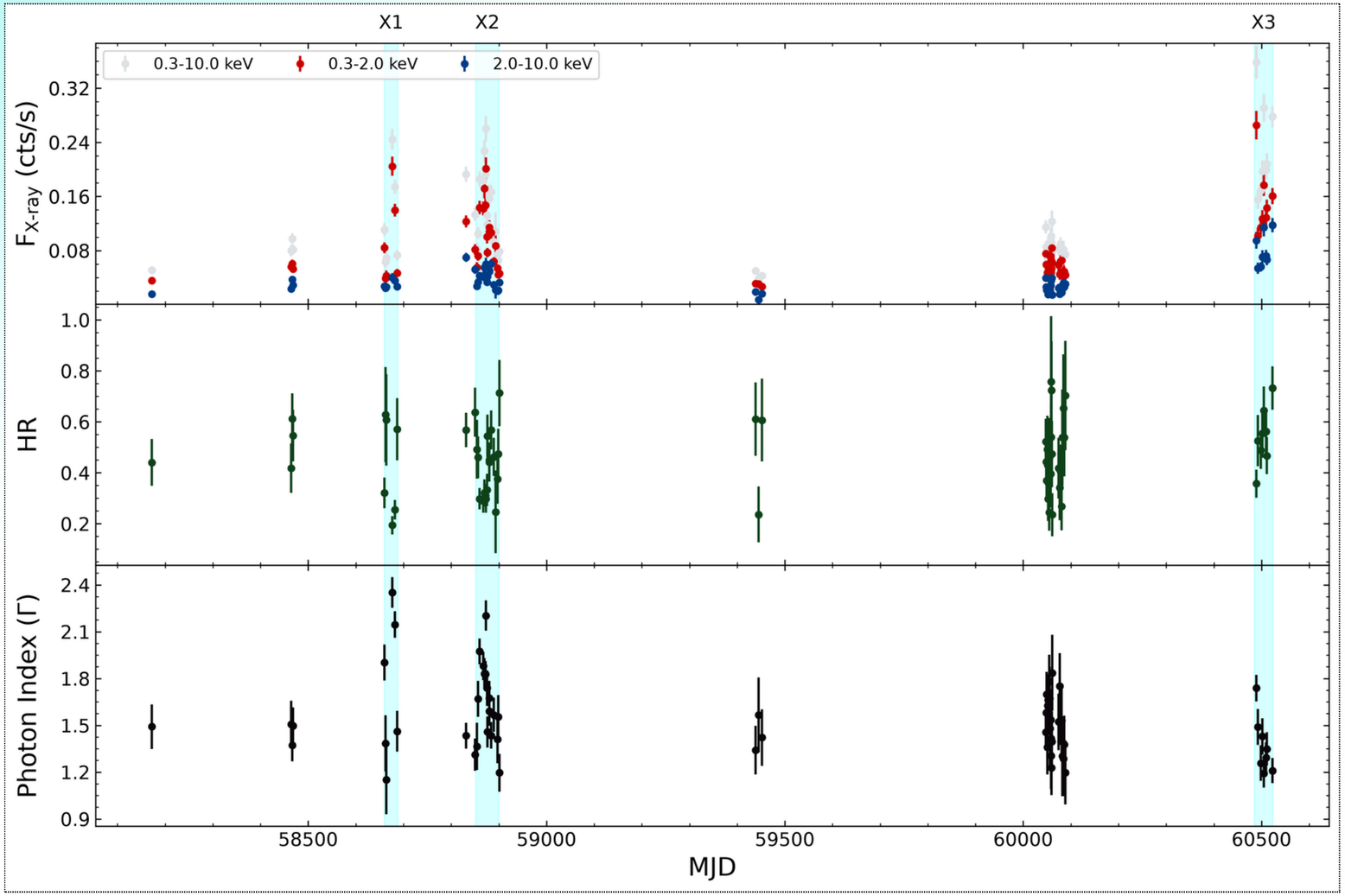
$$\mathrm{AIC}_c = 2k + C + \frac{2k(k+1)}{N-k-1}$$

Rejection criteria: $\Delta\mathrm{AIC}_c > 10$ relative to the minimum.

- No observation has $\Delta\mathrm{AIC}_c > 10$ for any model. All three are statistically acceptable.
- Best-fit model from Minimum $\mathrm{AIC}_c$:
  - **Power law: 47/64**
  - Log-parabola: 13/64
  - Broken power-law: 4/64

- X-ray emission is described by an absorbed power-law. No strong requirement for curvature or spectral breaks.
- Brightness variations are not accompanied by systematic hardening or softening on long timescales.

# X-ray Flare Selection



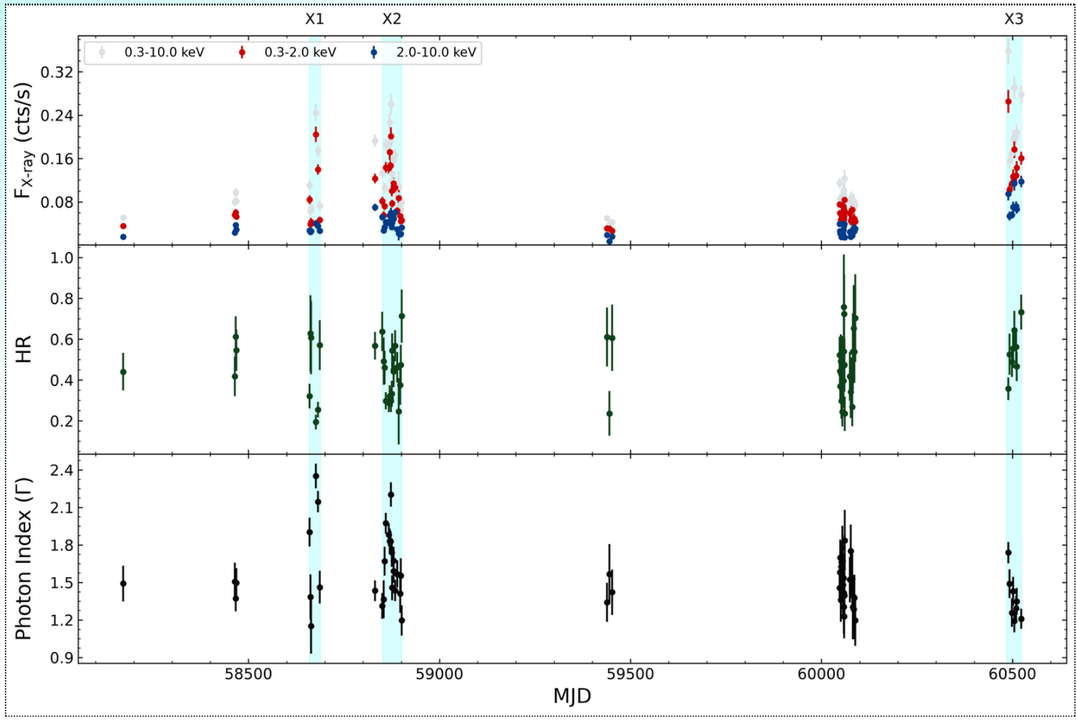

Flare Selection: Bayesian Blocks

$$F_{\text{Flare}} \geq 2\bar{F}$$

| Flare | Time Period |
|---|---|
| $X1$ | $58660.0 - 58688.0$ |
| $X2$ | $58852.0 - 58900.0$ |
| $X3$ | $60485.0 - 60524.0$ |

# X-ray Hardness Ratio

$$HR = \frac{H}{S}$$




| **Band** | **Rate** $(\mathrm{cts\,s^{-1}})$ | $\boldsymbol{F_{\mathrm{var}}}$ (%) |
|---|---|---|
| Soft (0.3-2 keV) | $0.085 \pm 0.006$ | $57.3 \pm 1.5$ |
| Hard (2-10 keV) | $0.038 \pm 0.003$ | $60.3 \pm 2.2$ |
| Full (0.3-10 keV) | $0.123 \pm 0.009$ | $55.9 \pm 1.2$ |

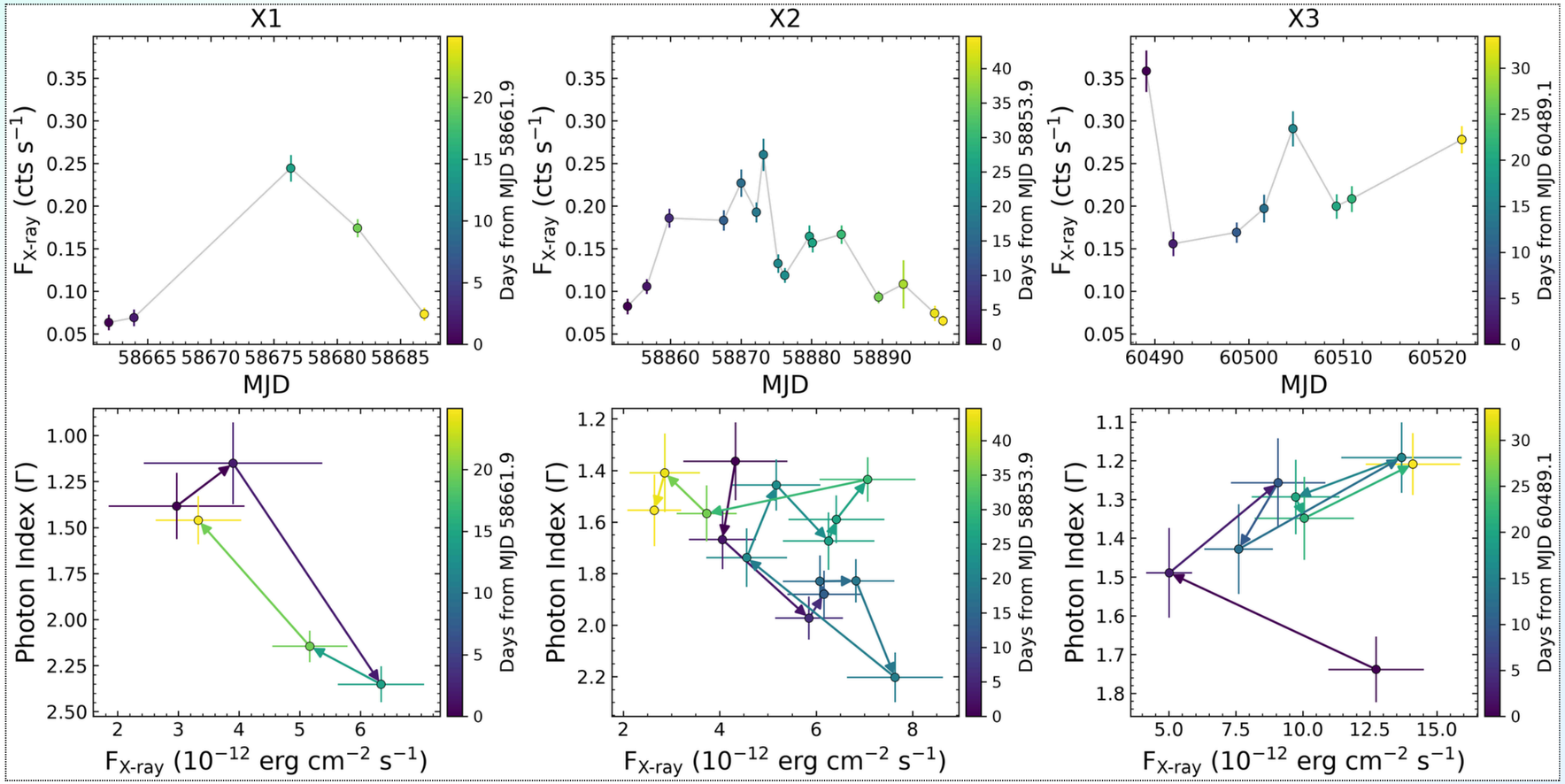
| Flare | $\overline{F}_{\mathrm{Soft}}$ $(\mathrm{cts\,s^{-1}})$ | $\overline{F}_{\mathrm{Hard}}$ $(\mathrm{cts\,s^{-1}})$ | HR | $\Gamma$ |
|---|---|---|---|---|
| X1 | $0.094 \pm 0.033$ | $0.030 \pm 0.003$ | $0.323 \pm 0.030$ | $1.97 \pm 0.09$ |
| X2 | $0.105 \pm 0.011$ | $0.039 \pm 0.003$ | $0.374 \pm 0.019$ | $1.71 \pm 0.04$ |
| X3 | $0.153 \pm 0.016$ | $0.085 \pm 0.009$ | $0.554 \pm 0.027$ | $1.34 \pm 0.06$ |

- The three flares harden monotonically: **Γ = 1.97 → 1.71 → 1.34** (X1 to X3).
- Systematic evolution from a soft flaring state (X1) to a hard flaring state (X3)

# X-ray Spectral Hysteresis

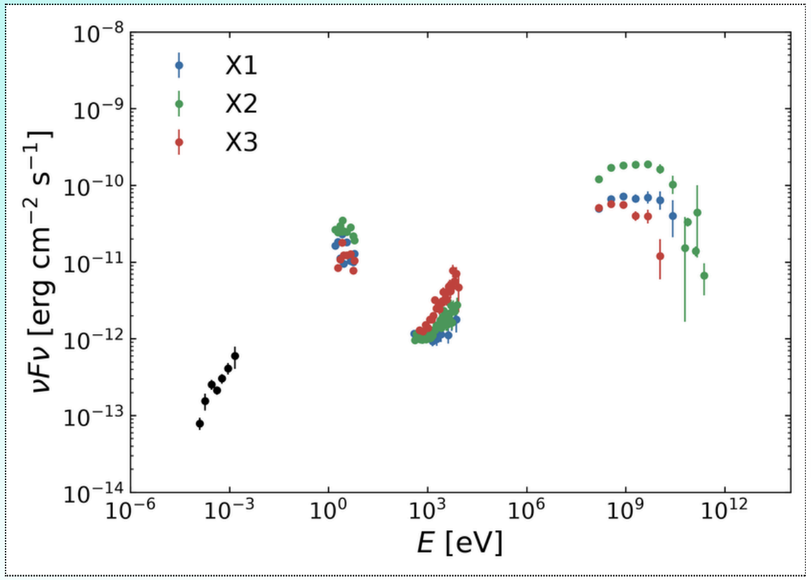
Loops in the flux vs Γ plane trace the competition between particle acceleration and radiative cooling.

- CW loop: soft lag, cooling dominated
- CCW loop: hard lag, acceleration timescale comparable to cooling




X1 is a CW cooling loop; X2 and X3 complex multi-loop trajectories, shifting acceleration/cooling balance.

# Broadband SEDs of the Flaring Epochs




## One-zone leptonic model - agnpy

- Single homogeneous spherical blob of radius $R_b$, uniform magnetic field B, isotropic relativistic electrons.

$$\delta_{\mathrm{D}} = [\Gamma(1 - \beta\cos\theta)]^{-1}$$

- Blob size constrained by causality, with $t_{var} \approx 9$ hrs from the shortest gamma-ray variability (**Prince et al. 2021**)

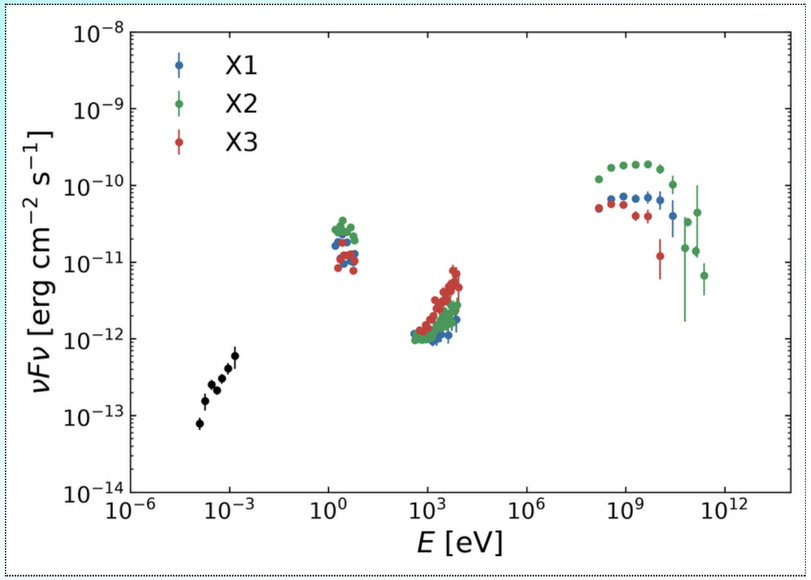
$$R_{\mathrm{b}} \lesssim c\,\delta_{\mathrm{D}}\,t_{\mathrm{var}}/1+z$$

- Electron energy distribution: **broken power law**

$$N(\gamma) = \begin{cases} k_e\,\gamma^{-p_1} & \gamma_{\mathrm{min}} \leq \gamma \leq \gamma_b \\ k_e\,\gamma_b^{p_2-p_1}\,\gamma^{-p_2} & \gamma_b < \gamma \leq \gamma_{\mathrm{max}} \end{cases}$$

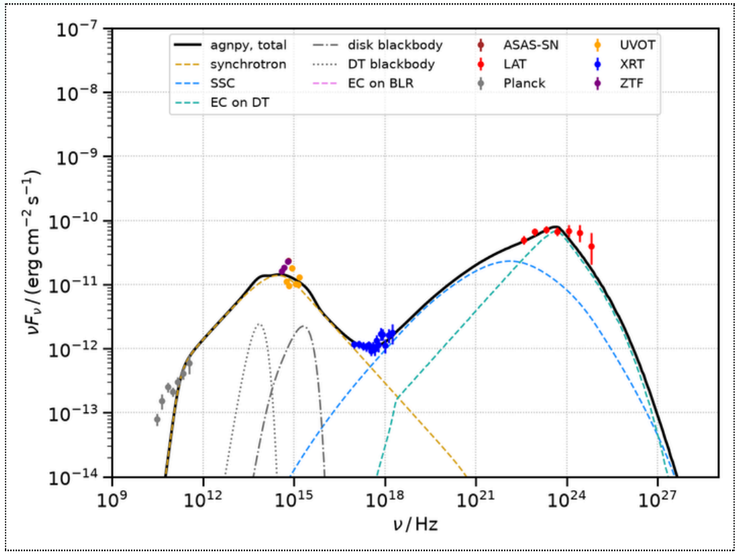
- Radiative components: synchrotron, SSC, and EC.

# Broadband SEDs of the Flaring Epochs

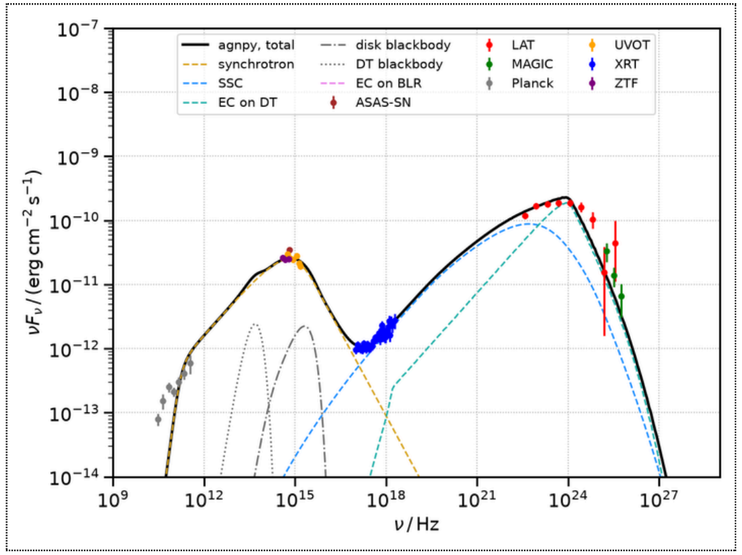



## One-zone leptonic model - agnpy

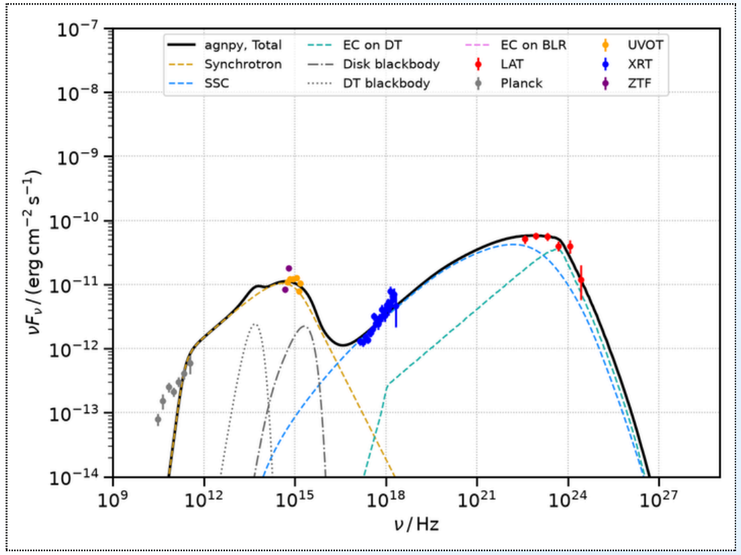
- Initial fit with iminuit, used to initialise MCMC with emcee; uniform priors for free parameters.
- Fixed: $\gamma_{min}$ = 10 (required to reproduce the valley between the two humps, **MAGIC Collaboration 2021**), $\gamma_{max}$ = $10^7$, and the EC component parameters.
- Emission-region location (r) left free initially; MCMC sampling converged to r ≈ 1.5 x $10^{19}$ cm, so r was fixed there in the final fit
- **Free parameters: $k_e$, $p_1$, $p_2$, $\gamma_b$, $\delta_D$, B**




**X1**




**X2**

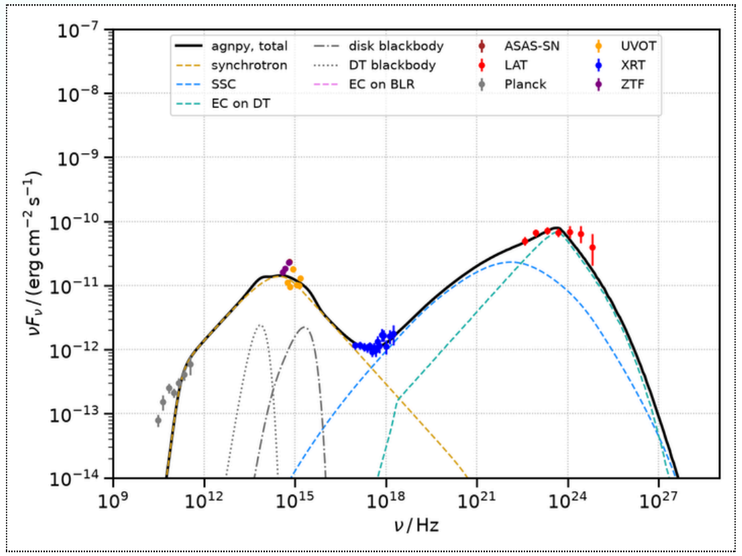



**X3**

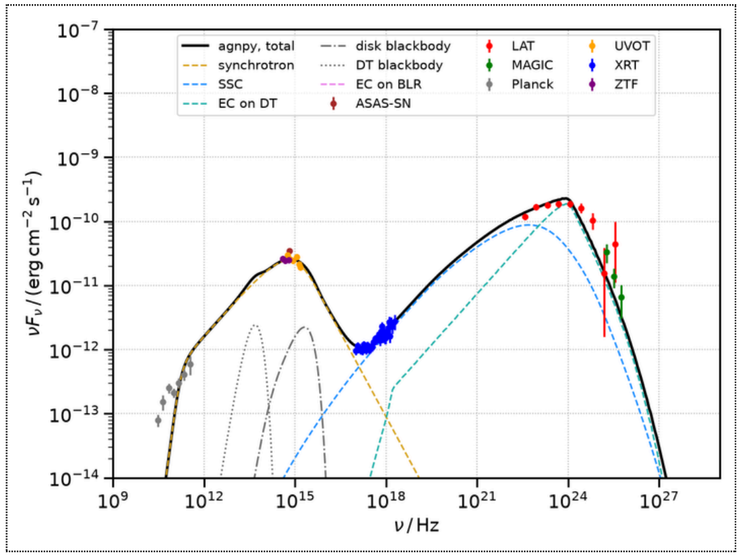
# Broadband SEDs of the Flaring Epochs

| Flare | $k_{\rm e}$ | $p_1$ | $p_2$ | $\gamma_{\rm b}$ | $\delta_{\rm D}$ | $B$ |
|---|---|---|---|---|---|---|
| X1 | $7.09^{+3.39}_{-2.46} \times 10^{-4}$ | $1.95^{+0.08}_{-0.08}$ | $4.05^{+0.08}_{-0.06}$ | $5.24^{+0.84}_{-0.68} \times 10^{3}$ | $34.20^{+1.43}_{-1.37}$ | $0.136^{+0.008}_{-0.007}$ |
| X2 | $3.33^{+1.13}_{-0.88} \times 10^{-4}$ | $1.94^{+0.04}_{-0.04}$ | $4.75^{+0.12}_{-0.10}$ | $9.23^{+1.11}_{-0.91} \times 10^{3}$ | $34.69^{+0.96}_{-1.01}$ | $0.113^{+0.004}_{-0.004}$ |
| X3 | $5.99^{+3.21}_{-2.06} \times 10^{-4}$ | $2.20^{+0.05}_{-0.06}$ | $4.87^{+0.10}_{-0.18}$ | $8.15^{+0.96}_{-0.97} \times 10^{3}$ | $28.01^{+1.18}_{-1.21}$ | $0.136^{+0.009}_{-0.008}$ |

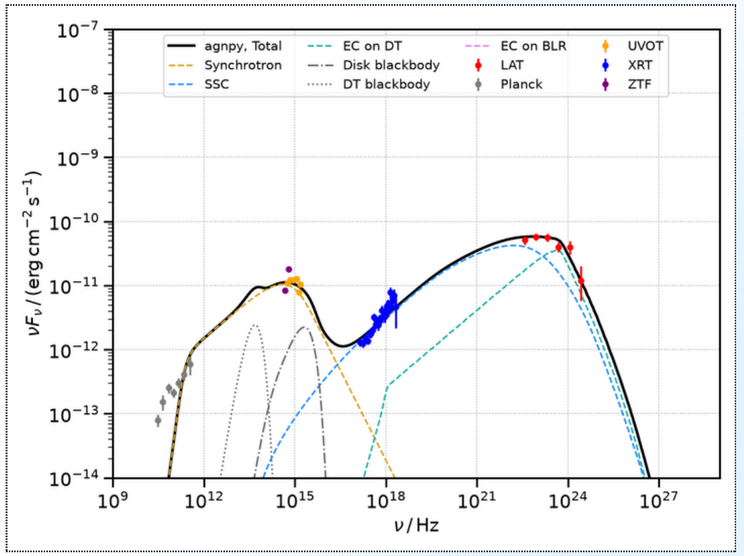
The  flaring is driven by changes in the particle population.




X1



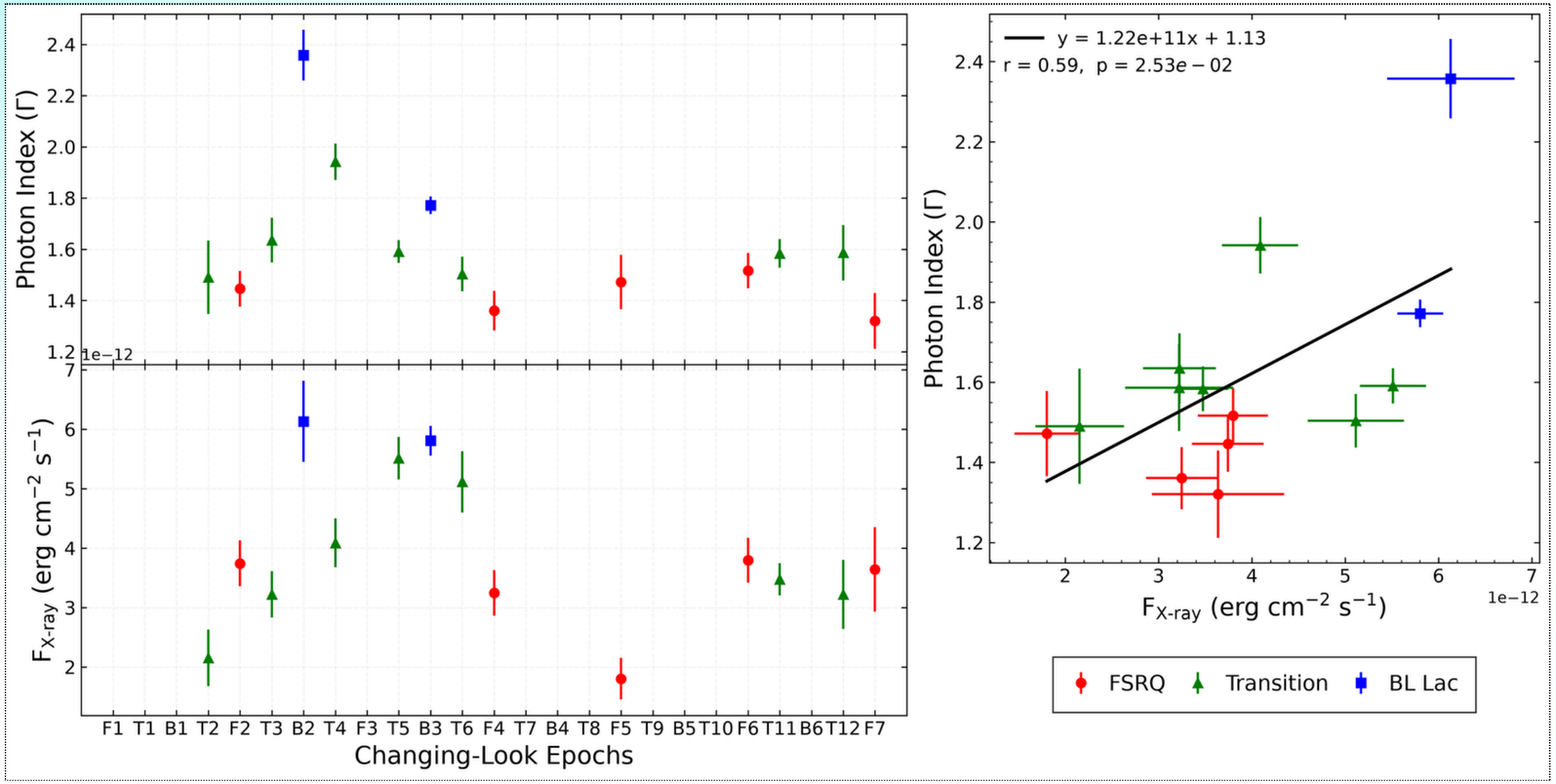

X2




X3

# Changing-Look States

Changing-Look epoch classifications is adopted from **Ren et al. (2024)**



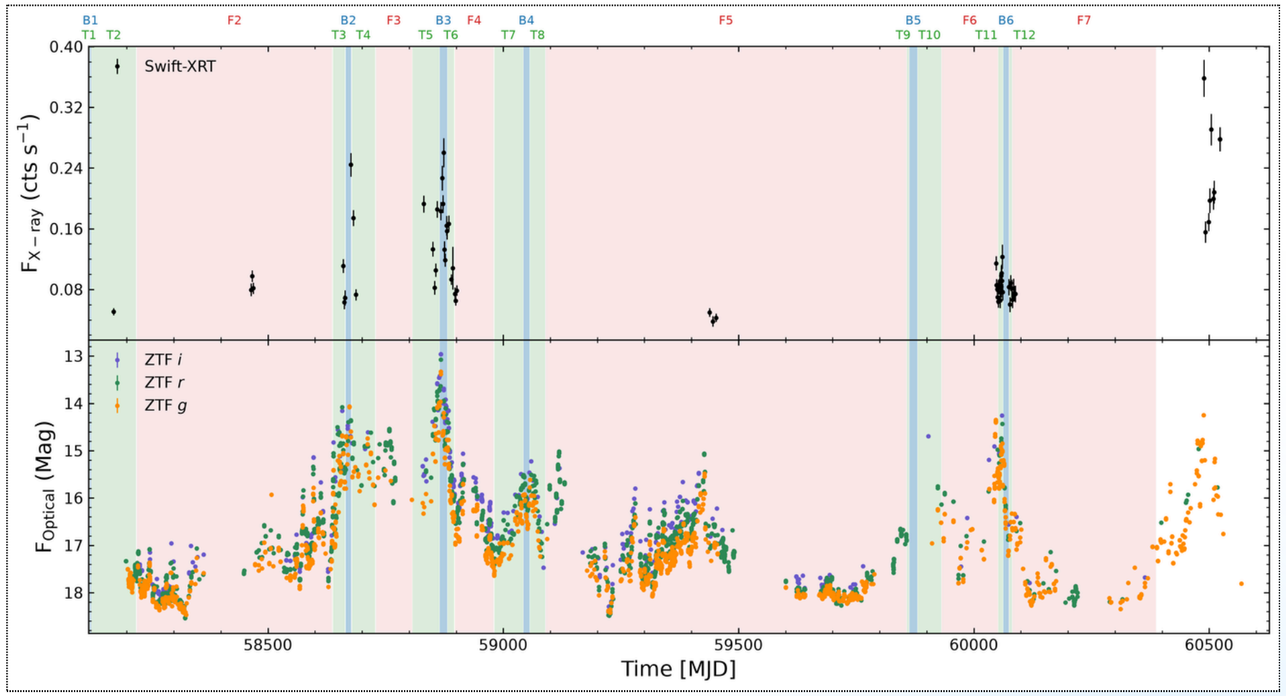

| **State** | $\boldsymbol{\Gamma_\gamma}$ (Ren+24) | $\boldsymbol{\Gamma_X}$ (this work) |
|---|---|---|
| FSRQ | $\gtrsim 2.2$ | $1.3 - 1.5$ |
| Transition | $2.0 - 2.2$ | $1.5 - 1.9$ |
| BL Lac | $\lesssim 2.0$ | $1.8 - 2.4$ |

- Within CL epochs, flux and $\Gamma_X$ correlate positively (r = 0.59, p = 0.025): **Softer-when-brighter** trend.

# X-ray Flares & CL States

- X1 overlaps T3, **B2**, T4
- X2 spans T5, **B3**, T6, F4
- X3 falls after the classified epoch range

In X1 and X2, $\Gamma_X$ softens into the BL Lac state from harder transition state and hardens again in the following transition state.




| **Flare** | $\Delta m_g$ (mag) |
|---|---|
| X1 | 1.73 |
| X2 | 3.65 |
| X3 | 2.10 |

- All three X-ray flares have bright optical counterparts (ZTF)
- The **FSRQ → BL Lac** transitions accompanied by ~1.5-2.5 mag optical flares (**Chand & Gopal-Krishna 2025**)

- BL Lac epochs are phases of elevated jet activity.
- The rising jet continuum dilutes the $Mg_{II}$ EW below the classification threshold, consistent with jet-continuum dilution of the broad lines.
- X3, the brightest flare has the hardest spectrum ($\Gamma_X$ = 1.34; $\Gamma_{X,Obs}$ = 1.2-1.7), FSRQ and Transition like CL epochs.

## Conclusions

- High-amplitude variability in all bands, with optical - γ-ray correlations.
- X-ray spectra mostly consistent with a simple power law ($AIC_c$ model selection).
- Spectral hysteresis: X1 is a CW cooling loop; X2 and X3 complex multi-loop trajectories, shifting acceleration/ cooling balance.
- Systematic hardening through the flares: **$\Gamma_X$ = 1.97 → 1.71 → 1.34** (X1 to X3).
- One-zone leptonic SEDs: X-rays go from synchrotron + IC (X1) to fully IC-dominated (X3); flares are particle driven.
- X-ray spectra separate the CL states (FSRQ hard, BL Lac soft); Flare X3 differ from the CL epochs.

# Thank You

npknavaneeth@gmail.com